Self-Immolative Hydroxybenzylamine Linkers for Traceless Protein Modification

Douglas A. Rose‡, Joseph W. Treacy‡, Zhongyue J. Yang, Jeong Hoon Ko*, K. N. Houk*, and Heather D. Maynard*

Department of Chemistry and Biochemistry and California NanoSystems Institute, University of California, Los Angeles, 607 Charles E. Young Drive East, Los Angeles, California 90095-1569, United States.

Supporting Information Placeholder

ABSTRACT: Traceless self-immolative linkers are widely used for the reversible modification of proteins and peptides. This article describes a new class of traceless linkers based on *ortho* or *para*-hydroxybenzylamines. The introduction of electron-donating substituents on the aromatic core stabilizes the quinone methide intermediate, thus providing a platform for payload release that can be modulated. To determine the extent to which the electronics affect the rate of release, we prepared a small library of hydroxybenzylamine linkers with varied electronics in the aromatic core, resulting in half-lives ranging from 20 to 144 hours. Optimization of the linker design was carried out with mechanistic insights from density functional theory (DFT) and the *in silico* design of an intramolecular trapping agent through the use of DFT and intramolecular distortion energy calculations. This resulted in development of a faster self-immolative linker with a half-life of 4.6 hours. To demonstrate their effectiveness as traceless linkers for bioconjugation, reversible protein-polyethylene glycol (PEG) conjugates with a model protein lysozyme were prepared, which have reduced protein activity but recover ≥94% activity upon traceless release of the polymer. This new class of linkers with tunable release rates expands the traceless linkers toolbox for a variety of bioconjugation applications.

▪ Introduction

Protein conjugation is a versatile tool that allows for the alteration of a protein's stability, activity, and functionality.[1] Protein-polymer conjugates are a useful application of this tool for therapeutically relevant proteins, often resulting in an increased stability and circulation time *in vivo*.[2] However, the covalent attachment of the polymer typically leads to a significant loss of activity compared to the unmodified counterpart, and in some cases, especially for proteins with large substrates, activity is reduced to zero.[3–5] To minimize such undesired effects, site-specific conjugation techniques can be employed to ensure that placement of the polymer is distant from the active site.[6] However, this is not broadly applicable to all proteins of interest and requires a tailor-made strategy for each protein, resulting in a significant investment of time and resources.

As an alternative strategy to circumvent activity loss, researchers place unstable linkages between the protein and the polymer.[7] These linkages slowly reverse to return any lost activity incurred by the presence of the attached polymer. Reversible linkages that release native protein are deemed traceless linkers. This conjugation strategy primarily targets either lysine or cysteine residues, and a variety of strategies have been developed for each.[8–13] Although traceless cysteine conjugation is very effective, the necessary free and accessible cysteine is not available across all proteins of interest. Comparatively, lysines, many of which are accessible for covalent modification, are highly prevalent across a wide range of proteins.[14]

One common traceless lysine conjugation strategy is the fluorenylmethoxycarbamate (Fmoc) linkage (Figure 1a).[11] Cleavage proceeds through a β-elimination pathway that is entirely mediated by pH. This strategy works well for applications requiring a slow passive release *in vivo*, well exemplified by Bempegaldesleukin, a long-acting interleukin-2 PEG conjugate that is currently in phase 3 clinical trials.[15] This passive release

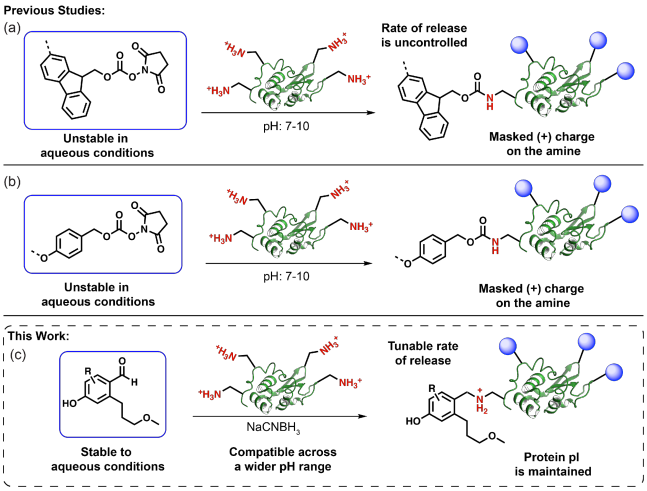

Figure 1. Strategies to prepare amine-reactive traceless bioconjugates: (a) fluorenylmethoxycarbamate (Fmoc) linker and (b) benzyl carbamate linker, compared to (c) hydroxybenzylamine linker.

does, however, limit the amount of control over both the rate and site of release. Conversely, the benzyl carbamate linkage (Figure 1b) is stable across a wide pH range and requires an initial deprotection of the aniline or phenol in order to proceed through the release mechanism.[9] Taking advantage of this reactivity, one can mask the phenol/aniline position with a diverse array of stimuli-responsive functionalities, adding a trigger-dependent release to the system.[16] This ensures the release is confined to locations where the stimulus is present, imparting a level of control to the system. While these linkers are used for stimuli-responsive release across a variety of bioconjugation applications, they are also used as passive traceless linkers within protein-polymer conjugation as demonstrated by Lonapegsomatropin, a long-acting

human growth hormone PEG conjugate that is currently undergoing phase 3 clinical trials.[17] Even though these strategies have been widely adopted, there are a few limitations creating room for further development. These include: (1) loss of the positive charge on the lysine residues that can destabilize the protein; (2) hydrolytic instability of carbonate precursors; and (3) high pH conditions required for conjugations.

In order to address these limitations, we developed a class of hydroxybenzylamine-based traceless linkers with tunable rates of release (Figure 1c). For the carbamate linkers, loss of CO_2 serves as the principal driving force for the amine release. Currently, conjugations using benzaldehyde derivatives lack such a driving force and are only utilized for permanent conjugations.[20,21,24] Yet, inspired by recent work showing the release of drugs containing tertiary amines and research showing the electronic effects on the strength of benzylic bonds,[18,19] we hypothesized that installing electron rich substituents on the aromatic core would facilitate dearomatization and stabilize the transient positive charge on the benzylic carbon to favor the 1,6-elimination of a primary amine.[19,25–27] Furthermore, by the choice of the functional groups on the aryl ring, we anticipated being able to tune the rate of release. The rate of release of the benzyl carbamate is based on the trigger used to unmask the phenol rather than the benzyl carbamate moiety itself, so this would be an additional advantage of the hydroxybenzylamine-based linkers. Furthermore, hydroxybenzylamines are conjugated to amines via reductive aminations on lysine and the N-terminal amine, which are carried out in an acidic to mildly basic pH solutions (Figure 1c). This complements the basic conditions used in the preparation of the benzyl carbamate linkers, and opens up the use of traceless linkers for proteins with isoelectric points (pI) between 7 – 9 that are incompatible with the carbamate conjugation conditions. Additionally, the resulting hydroxybenzylamine conjugate retains the positive charge on the amines, which has been shown to minimize denaturation and aggregation incurred by a shift in the isoelectric point and could be important for some proteins.[22,23] Herein, we describe the development of these hydroxybenzylamine-based traceless linkers experimentally and computationally, as well as an example application in the field of protein-polymer conjugation.

▪ Results and Discussion

Preparation and Release Studies of a Model Hydroxybenzylamine Library. To test the hypothesis that electron donating groups will allow for tunable amine release, we prepared a small library of model compounds using commercially available benzaldehydes and measured the release of an amine payload. The four benzaldehydes were chosen due to their varying levels of electron-donating abilities: benzaldehyde (**1**, $\sigma_p = 0.00$ for –H), dimethylbenzaldehyde (**2**, σ_p = -0.17 for each -Me), dimethoxybenzaldehyde (**3a**, σ_p = -0.27 for each -OMe), and dimethylaminobenzaldehyde (**4a**, σ_p = -0.83 for -NMe_2).[28] In the case of **1**, **2**, and **3a**, σ_p Hammett parameters were used, which have been found to be a good estimate for the *ortho*-substituent donating ability. These four model compounds were prepared via reductive amination with phenethylamine, which was chosen as a surrogate to lysine due to its low limit of detection when monitored by high-performance liquid chromatography (HPLC) for kinetic analysis.

The release studies were carried out using a 5 mM solution of the linker in a 1:1 mixture of methanol and Tris buffer (pH 7.4, 100 mM), where the appearance of phenethylamine was monitored via HPLC. As expected, the unsubstituted linker **1** showed no release over 25 days, whereas linker **2** had fully released the amine within the same time period ($t_{1/2}$: 144 hours) (See SI for experimental details). Increasing the electron donation of the substituents to the more electron-rich methoxy groups in linker **3a** resulted in faster release ($t_{1/2}$: 20 hours); however, further increasing the electron density with linker **4a** led to a slower release ($t_{1/2}$: 29 hours). First order rate constants calculated from this plot (Figure 2b) showed that the rate increased 6-fold between linkers **2** and **3a** (1.32×10^{-6} s^{-1} vs. 7.88×10^{-6} s^{-1} respectively, see Figure 2a). To better understand the mechanism of release, we prepared two additional linkers by methylating the phenols to obtain negative controls. As expected, this completely shut off the release for **3b**. However, linker **4b** did still release phenethylamine, albeit with a 17-fold reduction in the rate ($t_{1/2}$: 495 hours). This observation, along with a decreased rate of release under more acidic conditions (See SI page S59 for details), indicates the release pathway proceeds through an initial deprotonation of the phenol. Presumably, linker **4b** subverts the requisite deprotonation through a 1,6-elimination pathway, proceeding through an azaquinone methide intermediate to release the phenethylamine.

Excluding **4a**, linkers **1**, **2**, and **3a** clearly demonstrate that increasing the electron donation of the aryl substituents leads to a faster rate of release. The structural difference between **4a** and the other linkers could be the reason for this discrepancy; however, previous studies have shown the 1,4-elimination rate to be similar to that of the 1,6-elimination.[29] Yet, these studies were carried out with carbamate linkages and one could envision that the *ortho*-

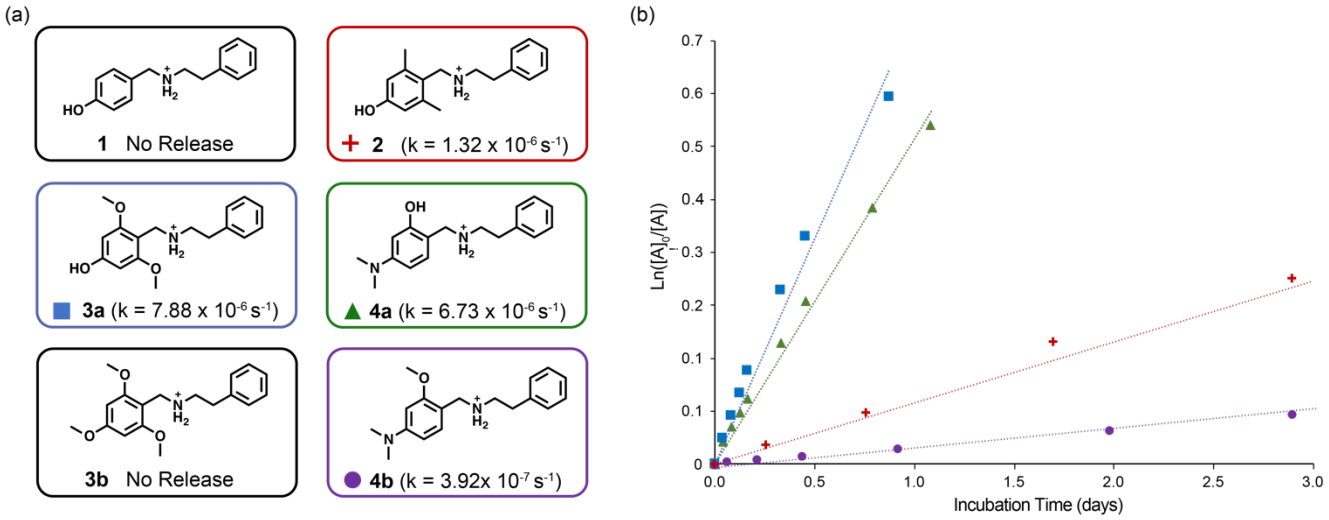

Figure 2. (a) Library of traceless linkers prepared for model release study with experimentally determined rate constants. (b) First order plot of phenethylamine release kinetics from the hydroxybenzylamine linker model compounds (n = 3, error bars are smaller than markers) carried out at 5 mM of linker in a 1:1 mixture of methanol and buffer (pH 7.4).

structure of this hydroxybenzylamine linker might facilitate hydrogen bonding between the benzylic amine and the phenol. This hydrogen bonding may affect the phenol's participation in the release mechanism, leading to the observed discrepancy. Additionally, the use of the σ_p values for linkers **2** and **3a** may not be perfectly translatable for the *ortho*-substituents, which would modify our expected trend. To investigate the reason for the seemingly anomalous behavior of **4a**, we examined the mechanism by density functional theory (DFT) calculations for the suite of hydroxybenzylamine linkers.

DFT and Intramolecular Distortion Energy Calculations for Linker Optimization. Free energy profiles (Figure 3) were calculated for the linkers beginning with an initial deprotonation (INT1) and a subsequent loss of the methylamine (TS1) to form the quinone methide intermediate (INT2). Interestingly, linker **2** had the lowest TS1 energy, contradicting our initial hypothesis that the release of the amine will correlate with the electronics on the aryl ring. When looking at TS2, it became clear that the quenching of the quinone methide intermediate was the rate-limiting step, indicating that the loss of the amine (TS1) is a reversible process. Experimentally, we observed formation of cyclic dimeric and trimeric species as the major products during the release studies. This suggested that the intermediate TS2 is quenched with the phenoxide and as a result, we quenched TS2 with phenoxide in the DFT calculations. Comparing the activation free energies ($\Delta G^{\ddagger}$) of these three linkers (Figure 3), we observed a correlation between the experimental $\Delta G^{\ddagger}$ and the calculated $\Delta G^{\ddagger}$. We found that there was a 0.5 kcal/mol difference between linkers **2** and **3a**, which aligns with the 1.1 kcal/mol difference we saw experimentally. Linker **4a** again deviated from the trend, showing a 0.2 kcal/mol difference compared to **2**. This discrepancy is likely due to the fact that linker **4a** proceeds through both the quinone methide and azaquinone methide intermediates, which in combination help to lower the $\Delta G^{\ddagger}$ even further. It is interesting to note the calculated phenol pK_a for linker **4a** (8.5) compared to linkers **2** and **3a** (7.3 and 6.3, respectively) was higher, which was caused in part by the intramolecular hydrogen bonding. This is not, however, the primary factor leading to the elevated activation energy of **4a**.

In order to prevent the reversibility of TS1 observed across all three linkers, we proposed that the addition of an intramolecular trapping agent would minimize the lifetime of INT2 and therefore limit any potential cross-reactivity. We hypothesized that the placement of an ethanol unit *ortho* to the hydroxybenzylamine would quench the quinone methide intermediate through an intramolecular hydration, forming a bicycle. However, prior to preparing this linker, we probed this hypothesis using DFT calculations. Exploration began with a pendant ethanol unit attacking the protonated quinone methide (TS2a), which was used as a model for the quinone methide hydrogen bonding with water. The $\Delta G^{\ddagger}$ of the transition state was calculated to be 15.1 kcal/mol, but examination of the transition state geometry showed that this six-membered transition state was highly strained due to the coplanarity among four of the six atoms involved (Figure 4).

To quantify this strain, intramolecular distortion energy calculations were developed (See SI page S198 for details), which showed a distortion energy of 12.1 kcal/mol for the ethanol arm (Table 1). To relieve strain in the transition state, an additional methylene unit was added to form the propanol pendant arm, which showed a decrease in $\Delta G^{\ddagger}$ by 3.1 kcal/mol and only a 1.0 kcal/mol increase in $-T\Delta S^{\ddagger}$. This difference in $\Delta G^{\ddagger}$ between the propanol and ethanol arms can be attributed to the distortion energy (DE) of the

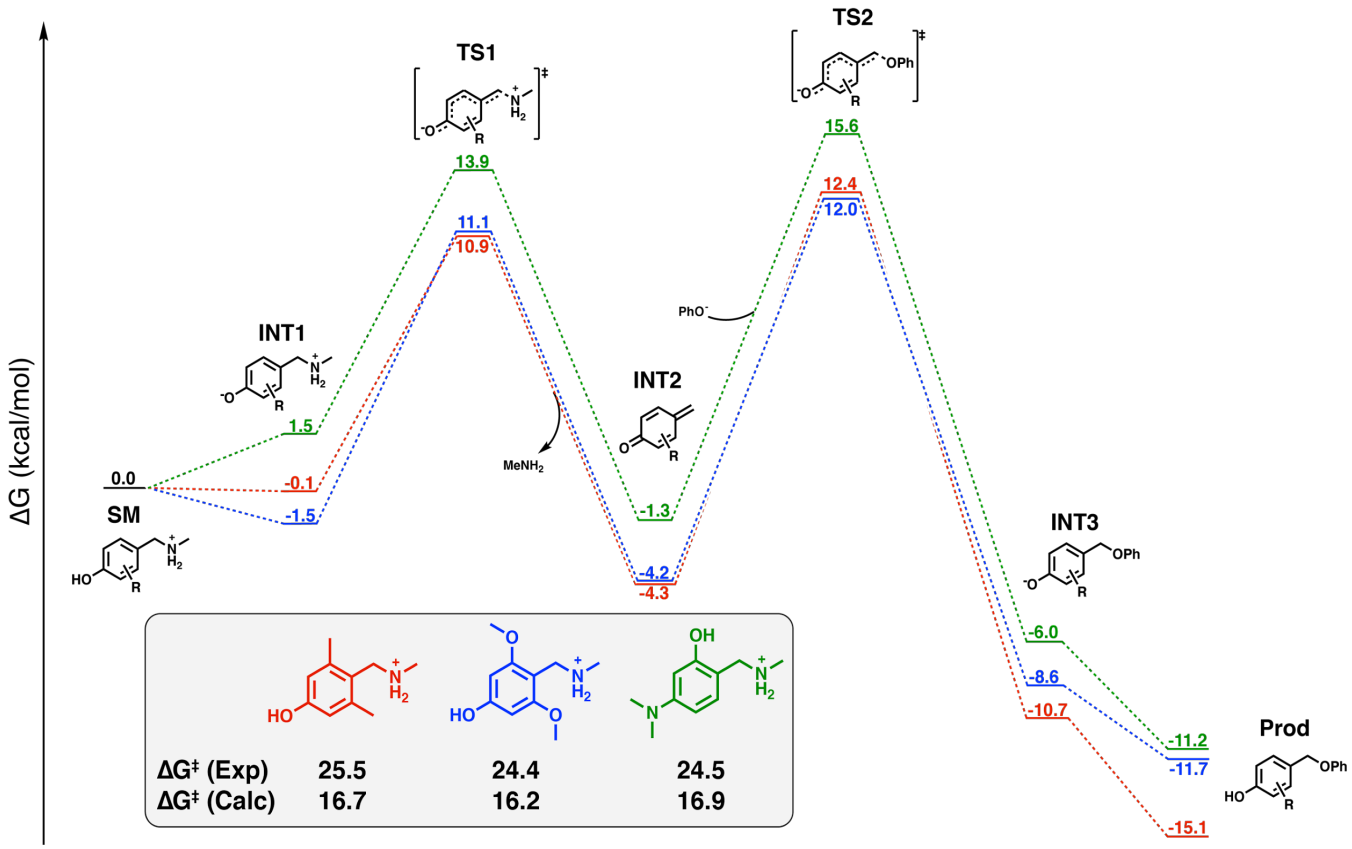

Figure 3. Reaction coordinate diagram of traceless amine release calculated using the M06-2X/aug-cc-pVTZ, CPCM(Water)//B3LYP-D3/6-31+G(d,p), CPCM(Water) level of theory. All energies are reported in units of kcal/mol (Calculated energies shown as calc in the inset, and experimental as exp). Linker **4a** undergoes a 1,4 elimination rather than the schematized 1,6 elimination (schematized as 1,6 elimination for clarity).

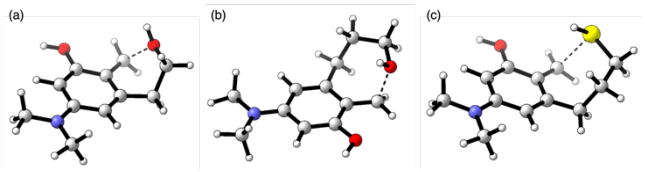

Figure 4. TS2a structures calculated at the B3LYP-D3/6-31+G(d,p), CPCM(Water) level of theory for entry 1 (a), entry 3 (b), and entry 5 (c) from Table 1.

two linkers, 6.5 kcal/mol and 12.1 kcal/mol, respectively. With the distortion partially overcome, we sought to enhance the nucleophilicity by screening the propanethiol arm as well as the ethyl methyl ether and propyl methyl ether arms. The addition of the pendant methyl ether groups lowered the $\Delta G^{\ddagger}$ relative to the alcohol counterparts, with a negligible impact on the distortion energies. Interestingly, the propanethiol pendant arm removed most of the distortion energy, likely due to the increased C-S bond length as compared to the C-O bond. This, in addition to the increased nucleophilicity of the thiol, further lowered the $\Delta G^{\ddagger}$ to 8.8 kcal/mol.

With the DFT calculations showing a significantly lower second transition state, linkers **5a** and **5b** were synthesized (See SI for the synthetic scheme and details). The propanol and propyl methyl ether arms were chosen instead of the propanethiol to eliminate the propensity for disulfide formation, which could lead to competing side reactions in a biological setting. The release kinetics of the resulting linkers were carried out as previously described and linkers **5a** and **5b** showed roughly a 4- and 5-fold rate enhancement compared to **4a** (Figure 5), respectively. The additional electronic donation from the alkyl substituent does not fully account for this large of a rate enhancement. This rate enhancement between **5a** and **5b** can be attributed to the increased nucleophilicity of the methoxy group compared to the alcohol, which aligns well with our DFT calculations. In order to confirm that the intramolecular trapping arm was in fact quenching INT2a rather than undergoing a nucleophilic substitution reaction, linker **5c** (Figure 5) was prepared as a negative control. The release kinetics of **5c** showed a 13-fold reduction in the rate of phenethylamine release compared to **5b**, which shows similar trend to **4b** vs. **4a** (17-fold reduction), confirming that these linkers are proceeding primarily through a quinone methide intermediate. Additionally, the successful rate enhancement of **5a** and **5b** compared to **4a** supports our

Table 1. Intramolecular trapping of the quinone methide comparison.

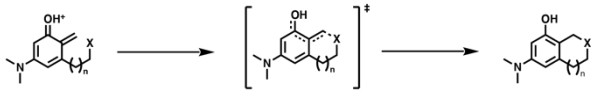

Entry	n	X	$\Delta G^{\ddagger}$ (kcal/mol)	DE (kcal/mol)	$-T\Delta S^{\ddagger}$ (kcal/mol)
1	1	OH	15.1	12.1	1.7
2	1	OMe	13.9	11.8	2.2
3	2	OH	12.0	6.5	2.7
4	2	OMe	10.1	6.8	2.9
5	2	SH	8.8	0.6	2.6

a. Transition state energies for the reaction of the pendant arm with the protonated quinone methide calculated at the M06-2X/aug-cc-pVTZ, CPCM(Water)//B3LYP-D3/6-31+G(d,p), CPCM(Water) level of theory. See SI for details on distortion energy calculations.

calculations that indicate that TS2 is the rate-determining step in the release mechanism.

Preparation of Traceless Lysozyme-PEG Conjugates. To demonstrate this approach as useful traceless linkers for protein conjugation, **6**, **7**, and **8** (Figure 6) were synthesized (See SI for synthesis). These three linkers were designed with varying electronics to modulate the rate of release, along with the incorporation of the propyl methyl ether intramolecular trapping arm to minimize any reversibility. Masking of the phenol was necessary to limit any unintended release during the polymer conjugation and purification steps. Thus, for the stimuli-responsive trigger, we chose an acetal protecting group that can be quickly removed in acidic conditions where the hydroxybenzylamine linker is more stable. We designed the linkers to initially undergo reductive amination onto the protein followed by a copper-mediated azide alkyne cycloaddition with an azide-containing PEG species (5 kDa mPEG-N_3) to afford the protein-PEG conjugates (Figure 7). This system was designed this way in order to aid in the characterization of the intermediates, where the modified protein could be easily characterized via LCMS to ensure the linkers were conjugated as intended. Lysozyme (Lyz) was chosen as the model protein because it has 6 accessible lysine residues along with the N-terminal amine, and the activity assay is well-established.[30]

Reductive amination conditions were initially screened varying the choice of buffer, pH, concentration, and benzaldehyde equivalence (See SI, Table on Page S59). It was found that 0.1 M borate buffer at pH 8.0 using 3.5 equiv. of linker per amine (20 equiv. to Lyz) produced a high degree of modification (up to 5

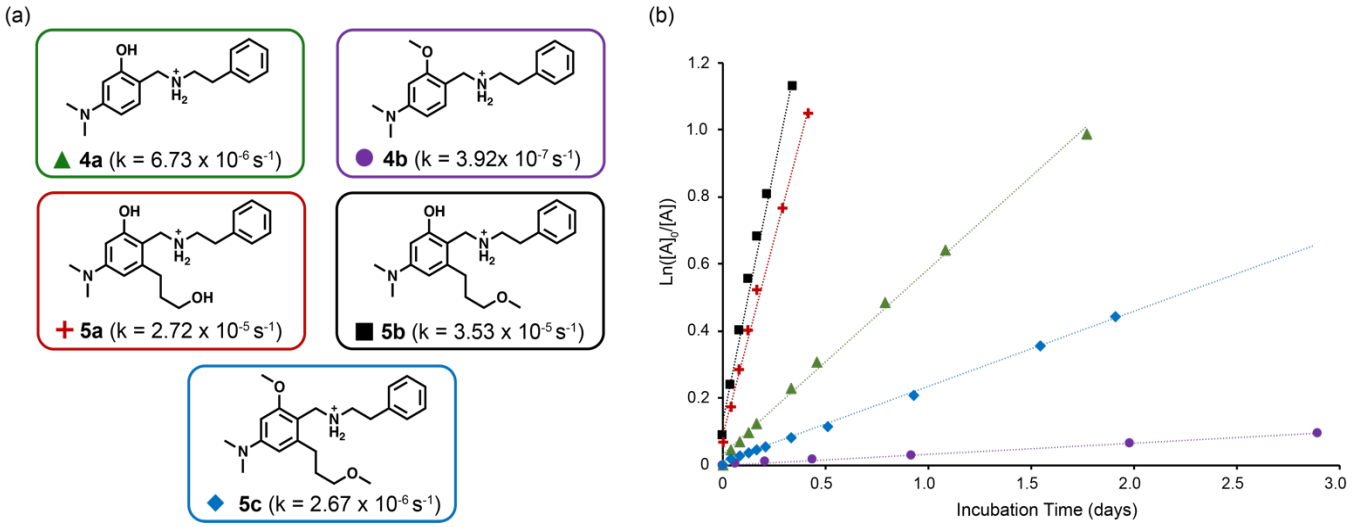

Figure 5. (a) Dimethylamino family of traceless linkers with and without an intramolecular trapping agent along with experimentally determined rate constants. (b) First order plot of phenethylamine release kinetics from the hydroxybenzylamine linker model compounds (n = 3, error bars are smaller than markers) carried out at 5 mM of linker in a 1:1 mixture of methanol and buffer (pH 7.4).

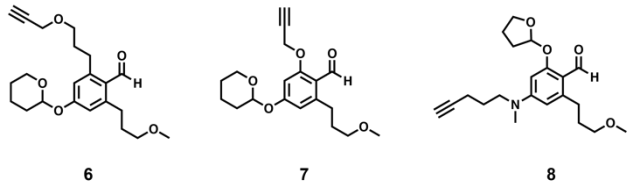

Figure 6. Traceless linkers prepared for protein conjugation.

linkers attached after 48 h) as measured by LCMS without deprotection of the acetal group. Additionally, lower pH that is reported to favor modification at the N-terminus over the lysine residues was found to preferentially produce a single amine modification.[31] Unsurprisingly, under more acidic conditions the cyclic acetal groups were unstable and in turn allowed for the self-immolative release, decreasing the conjugation efficiency. The choice of an alternative masking agent on the phenol that is stable to the acidic conditions would likely increase the efficiency of the reaction at lower pH's.

Targeting a high percent modification with an excess of **7** and **8** afforded perfunctionalized lysozyme species within 72 hours modifying five and three amines, respectively. however, reaction with **6** proved to be quite sluggish and only one amine was modified over 72 hours. Attempts to increase the degree of modification with **6**, including the addition of catalytic aniline and elevated temperatures, were employed, yet full conversion to the monofunctionalized lysozyme was never observed.[32] This decreased reactivity is likely due to the increased steric bulk around the benzaldehyde and the increased hydrophobicity compared to **7** and **8**, which in turn decreased the rate of imine formation relative to the competing benzaldehyde reduction.

Therefore, the two lysozyme-linker conjugates were carried forward, and the copper mediated azide-alkyne cycloaddition was undertaken using previously reported conditions to form the mPEG-linker-Lyz conjugates.[33] The copper-click conjugation to mPEG-N_3 was complete within 12 hours. Interestingly, Lyz-**7** formed multi-PEGylated species, while Lyz-**8** preferentially formed the mono-PEGylated conjugate under the same conditions (See SI for details). We believe the competing azaquinone release mechanism reduces the stability of Lyz-**8**, which in turn limits the conjugation efficiency. In order to more accurately compare the rate of lysozyme release between the two linkers, the mono-PEGylated lysozyme conjugates were isolated for both Lys-**7** and Lys-**8** via size exclusion chromatography. These monoPEGylated lysozyme conjugates were subsequently deprotected under acidic conditions (pH 4.0) to remove the cyclic acetal protecting group, prior to beginning the release assay.

Traceless Release of Lysozyme and Activity Recovery Studies. The traceless release of Lyz was monitored from the two deprotected mono-PEGylated lysozyme conjugates (Figure 8) in

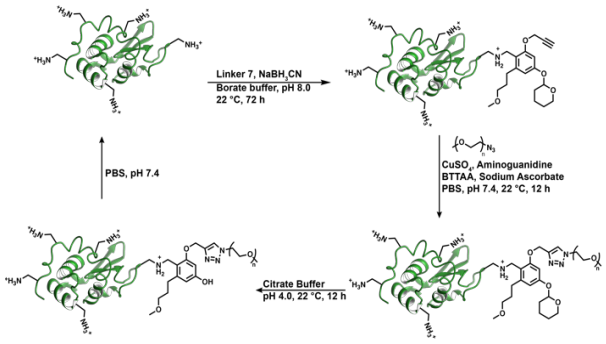

Figure 7. Representative stepwise protein conjugation scheme for the preparation of traceless mPEG-**7**-Lyz conjugate.

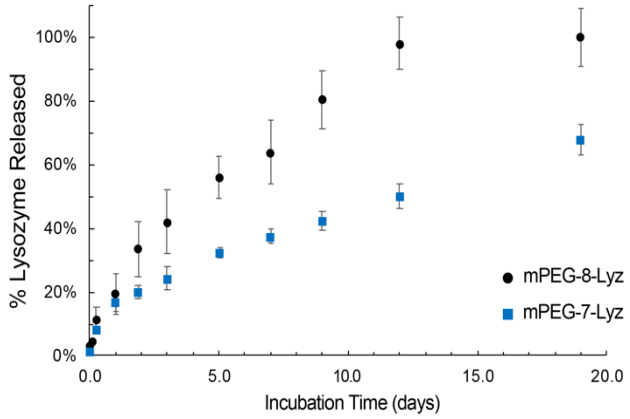

Figure 8. Traceless release of lysozyme from Lyz-mPEG conjugates in phosphate buffer (pH 7.4) monitored via HR-LCMS. Note that each conjugate has only 1 PEG chain attached.

phosphate buffer at pH 7.4. The kinetics were obtained by determining the amount of free Lyz in solution using HR-LCMS, thus ensuring that native Lyz was released. The mPEG-**8**-Lyz conjugate reached 98% release within 12 days, while mPEG-**7**-Lyz showed 50% release within the same time period. The trend between the electron donation into the aromatic core and the rate of release aligns with our model system; however, a dramatic decrease in the rate was observed between the small molecules and protein-polymer conjugates. This is not unexpected with a large, bulky protein-polymer conjugate versus a small molecule probe. Yet, importantly, the rate of release was altered just by changing the linker design. A more detailed study of conjugation rates, versus the numbers of polymers, the polymer structure, protein size, etc. is currently in progress.

The lysozyme activity for each of the mPEG-Lyz conjugates was compared before and after traceless release as a percent of the positive control (fresh unmodified lysozyme). Lysozyme activity was determined through the cell lysis of FITC labeled Gram-positive *Micrococcus luteus* in the EnzChek lysozyme activity assay (Figure 9). mPEG-**7**-Lyz showed a 28% reduction in activity with one polymer attached that was restored to 97% upon traceless release. Similarly, the mPEG-**8**-Lyz showed a 34% reduction in activity that was restored to 94% upon release. This demonstrates that the PEG is being removed and the lysozyme is not adversely affected by the conjugation procedure. An increase in the PEG molecular weight or degree of PEGylation would be expected to further amplify the activity difference before and after traceless release.

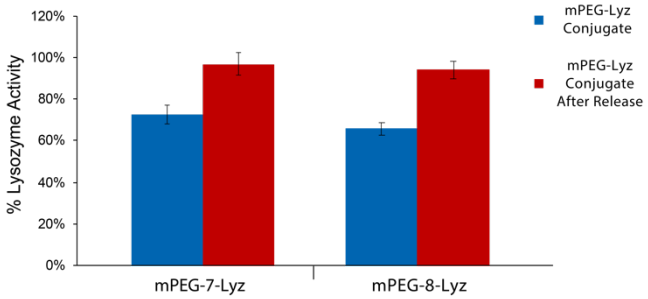

Figure 9. Lysozyme activity assay comparison between each Lyz conjugate before (blue) and after (red) traceless release.

This work focused on the proof of concept for the design and implementation of this new class of traceless linker. We demonstrate the applicability of the hydroxybenzylamine linkers for use in traceless protein-polymer conjugation using the model

protein lysozyme. Additional studies will need to be undertaken with a range of proteins, including therapeutically relevant ones, in order to investigate the generality of the approach. We anticipate that further adoption into the field of stimuli-responsive, self-immolative linkers is possible. The acetal protecting group on the phenol was chosen as a model stimuli-responsive functional group in this study, which could easily be replaced with other stimuli-responsive groups to impart a stimuli-specific release in the system, adding an additional layer of control. A site-specific trigger in addition to the variable rate of release would allow researchers to control the location and rate of release leading to the design of next generation therapeutics, and these studies are underway. Stimuli-triggered switching of protein activity has long been of interest in biotechnology,[34] and the strategy has potential for applications such as oral protein delivery,[35] and targeted drug delivery, reducing off-target effects. The results in this paper suggest that benzaldehydes may be utilized in this context.

▪ Conclusions

A small library of hydroxybenzylamine linkers was prepared with varying electron density that gave half-lives of 20 to 144 hours, or no release at all. DFT calculations and experimental studies helped elucidate the mechanism of release, which revealed that the loss of the amine-based payload was a reversible step. Based on this mechanistic insight, an intramolecular trapping arm was designed to quench the quinone methide intermediate. *In silico* design of the nucleophilic pendant arm decreased the $\Delta G^{\ddagger}$ of the quinone methide attack by 5.0 kcal/mol, which can largely be attributed to the reduction in distortion energy of the transition state. The benzaldehyde linkers containing these designed pendant arms were synthesized (**5a** and **5b**), resulting in faster half-lives by 7 and 6 hours, respectively.

Using insights gained from the small molecule hydroxybenzylamine kinetics experiments and DFT calculations, benzaldehyde substrates containing the intramolecular trapping arm and an alkyne click handle were synthesized for application in traceless protein-PEG conjugates. Lysozyme was chosen as a model enzyme and the conjugates were prepared through an initial reductive amination reaction, followed by a copper-click cycloaddition, and subsequent deprotection of the acetal to afford the mono-PEGylated lysozyme conjugates. As expected, with the polymer attached, the conjugates had reduced enzymatic activity that was subsequently restored upon release of PEG. The rate of traceless release varied between the two conjugates with half-lives of 5 and 12 days depending on the electronics of the linker. This modularity in the rate of release and linker design makes this new class of traceless linkers a useful addition to the bioconjugation toolbox.

ASSOCIATED CONTENT

Supporting Information

The Supporting Information is available free of charge on the ACS Publications website.

Experimental details, NMR spectra, supplementary figures, and coordinates of computed structures (PDF).

AUTHOR INFORMATION

Corresponding Authors

*maynard@chem.ucla.edu
*houk@chem.ucla.edu
*jk16@caltech.edu

Author Contributions

‡D.A.R. and J.W.T. contributed equally to this work.

Notes

The authors declare no competing financial interest.

ACKNOWLEDGMENT

This work was funded by the National Institute of Health (NIBIB R01EB020676) and the National Science Foundation (CHE-2003946). The AV500 NMR was supported by the National Science Foundation under equipment grant number CHE-1048804. This work used computational and storage services associated with the Hoffman2 Shared Cluster provided by UCLA Institute for Digital Research and Education's Research Technology Group. We thank Professor Sanzhong Luo and Siyuan Liu for their assistance with the pK_a calculations.

REFERENCES

(1) Gunnoo, S. B.; Madder, A. Bioconjugation – Using Selective Chemistry to Enhance the Properties of Proteins and Peptides as Therapeutics and Carriers. *Org. Biomol. Chem*. **2016**, 14, 8002–8013.

(2) Pelegri-O'Day, E. M.; Lin, E.-W.; Maynard, H. D. Therapeutic Protein–Polymer Conjugates: Advancing Beyond PEGylation. *J. Am. Chem. Soc*. **2014**, 136, 14323–14332.

(3) Morgenstern, J.; Gil Alvaradejo, G.; Bluthardt, N.; Beloqui, A.; Delaittre, G.; Hubbuch, J. Impact of Polymer Bioconjugation on Protein Stability and Activity Investigated with Discrete Conjugates: Alternatives to PEGylation. *Biomacromolecules* **2018**, 19, 4250–4262.

(4) Lucius, M.; Falatach, R.; McGlone, C.; Makaroff, K.; Danielson, A.; Williams, C.; Nix, J. C.; Konkolewicz, D.; Page, R. C.; Berberich, J. A. Investigating the Impact of Polymer Functional Groups on the Stability and Activity of Lysozyme–Polymer Conjugates. *Biomacromolecules* **2016**, 17, 1123–1134.

(5) Tucker, B. S.; Stewart, J. D.; Aguirre, J. I.; Holliday, L. S.; Figg, C. A.; Messer, J. G.; Sumerlin, B. S. Role of Polymer Architecture on the Activity of Polymer–Protein Conjugates for the Treatment of Accelerated Bone Loss Disorders. *Biomacromolecules* **2015**, 16, 2374–2381.

(6) Wang, Y.; Wu, C. Site-Specific Conjugation of Polymers to Proteins. *Biomacromolecules* **2018**, 19, 1804–1825.

(7) Gong, Y.; Leroux, J.-C.; Gauthier, M. A. Releasable Conjugation of Polymers to Proteins. *Bioconjug. Chem*. **2015**, 26, 1172–1181.

(8) Diehl, K. L.; Kolesnichenko, I. V.; Robotham, S. A.; Bachman, J. L.; Zhong, Y.; Brodbelt, J. S.; Anslyn, E. V. Click and Chemically Triggered Declick Reactions through Reversible Amine and Thiol Coupling via a Conjugate Acceptor. *Nat. Chem*. **2016**, 8, 968–973.

(9) Lee, S.; Greenwald, R. B.; McGuire, J.; Yang, K.; Shi, C. Drug Delivery Systems Employing 1,6-Elimination: Releasable Poly(Ethylene Glycol) Conjugates of Proteins. *Bioconjug. Chem*. **2001**, 12, 163–169.

(10) Zhao, H.; Yang, K.; Martinez, A.; Basu, A.; Chintala, R.; Liu, H.-C.; Janjua, A.; Wang, M.; Filpula, D. Linear and Branched Bicin Linkers for Releasable PEGylation of Macromolecules: Controlled Release in Vivo and in Vitro from Mono- and Multi-PEGylated Proteins. *Bioconjug. Chem*. **2006**, 17, 341–351.

(11) Peleg-Shulman, T.; Tsubery, H.; Mironchik, M.; Fridkin, M.; Schreiber, G.; Shechter, Y. Reversible PEGylation: A Novel Technology To Release Native Interferon A2 over a Prolonged Time Period. *J. Med. Chem*. **2004**, 47, 4897–4904.

(12) Garman, A. J.; Barret Kalindjian, S. The Preparation and Properties of Novel Reversible Polymer-Protein Conjugates 2-ω-

Methoxypolyethylene (5000) Glycoxymethylene-3-Methylmaleyl Conjugates of Plasminogen Activators. *FEBS Lett*. **1987**, 223, 361–365.

(13) Brocchini, S.; Godwin, A.; Balan, S.; Choi, J.; Zloh, M.; Shaunak, S. Disulfide Bridge Based PEGylation of Proteins. *Adv. Drug Deliv. Rev*. **2008**, 60, 3–12.

(14) Hacker, S. M.; Backus, K. M.; Lazear, M. R.; Forli, S.; Correia, B. E.; Cravatt, B. F. Global Profiling of Lysine Reactivity and Ligandability in the Human Proteome. *Nat. Chem*. **2017**, 9, 1181–1190.

(15) Bossard, M. J.; Ali, C. F.; Liu, X.; Charych, D. H.; Zappe, H.; Wang, Y.; Huang, J. Conjugates of an Il-2 Moiety and a Polymer. WO2012065086A1, May 18, 2012.

(16) Peterson, G. I.; Larsen, M. B.; Boydston, A. J. Controlled Depolymerization: Stimuli-Responsive Self-Immolative Polymers. *Macromolecules* **2012**, 45, 7317–7328.

(17) Rau, H.; Kindermann, S.; Lessmann, T.; RASMUSSEN, G. N.; Hersel, U.; Wegge, T.; Sprogøe, K. Pegylated Recombinant Human Growth Hormone Compounds. WO2009133137A2, November 5, 2009.

(18) Staben, L. R.; Koenig, S. G.; Lehar, S. M.; Vandlen, R.; Zhang, D.; Chuh, J.; Yu, S.-F.; Ng, C.; Guo, J.; Liu, Y.; Fourie-O'Donohue, A.; Go, M.; Linghu, X.; Segraves, N. L.; Wang, T.; Chen, J.; Wei, B.; Phillips, G. D. L.; Xu, K.; Kozak, K. R.; Mariathasan, S.; Flygare, J. A.; Pillow, T. H. Targeted Drug Delivery through the Traceless Release of Tertiary and Heteroaryl Amines from Antibody–Drug Conjugates. *Nat. Chem*. **2016**, 8, 1112–1119.

(19) Schmid, K. M.; Jensen, L.; Phillips, S. T. A Self-Immolative Spacer That Enables Tunable Controlled Release of Phenols under Neutral Conditions. *J. Org. Chem*. **2012**, 77, 4363–4374.

(20) Sun, G.; Fang, H.; Cheng, C.; Lu, P.; Zhang, K.; Walker, A. V.; Taylor, J.-S. A.; Wooley, K. L. Benzaldehyde-Functionalized Polymer Vesicles. *ACS Nano* **2009**, 3, 673–681.

(21) Liu, Y.; Lee, J.; Mansfield, K. M.; Ko, J. H.; Sallam, S.; Wesdemiotis, C.; Maynard, H. D. Trehalose Glycopolymer Enhances Both Solution Stability and Pharmacokinetics of a Therapeutic Protein. *Bioconjug. Chem.* **2017**, 28, 836–845.

(22) Kinstler, O. B.; Brems, D. N.; Lauren, S. L.; Paige, A. G.; Hamburger, J. B.; Treuheit, M. J. Characterization and Stability of N-Terminally PEGylated RhG-CSF. *Pharm. Res.* **1996**, 13, 996–1002.

(23) Baker, S. L.; Murata, H.; Kaupbayeva, B.; Tasbolat, A.; Matyjaszewski, K.; Russell, A. J. Charge-Preserving Atom Transfer Radical Polymerization Initiator Rescues the Lost Function of Negatively Charged Protein–Polymer Conjugates. *Biomacromolecules* **2019**, 20, 2392–2405.

(24) Samanta, D.; McRae, S.; Cooper, B.; Hu, Y.; Emrick, T.; Pratt, J.; Charles, S. A. End-Functionalized Phosphorylcholine Methacrylates and Their Use in Protein Conjugation. *Biomacromolecules* **2008**, 9, 2891–2897.

(25) Alouane, A.; Labruère, R.; Le Saux, T.; Schmidt, F.; Jullien, L. Self-Immolative Spacers: Kinetic Aspects, Structure–Property Relationships, and Applications. *Angew. Chem. Int. Ed.* **2015**, 54, 7492–7509.

(26) Muranaka, K.; Ichikawa, S.; Matsuda, A. Development of the Carboxamide Protecting Group, 4-(Tert-Butyldimethylsiloxy)-2-Methoxybenzyl. *J. Org. Chem*. **2011**, 76, 9278–9293.

(27) Weinert, E. E.; Dondi, R.; Colloredo-Melz, S.; Frankenfield, K. N.; Mitchell, C. H.; Freccero, M.; Rokita, S. E. Substituents on Quinone Methides Strongly Modulate Formation and Stability of Their Nucleophilic Adducts. *J. Am. Chem. Soc*. **2006**, 128, 11940–11947.

(28) Hansch, Corwin.; Leo, A.; Taft, R. W. A Survey of Hammett Substituent Constants and Resonance and Field Parameters. *Chem. Rev*. **1991**, 91, 165–195.

(29) Erez, R.; Shabat, D. The Azaquinone-Methide Elimination: Comparison Study of 1,6- and 1,4-Eliminations under Physiological Conditions. *Org. Biomol. Chem*. **2008**, 6, 2669–2672.

(30) Masuda, T.; Ide, N.; Kitabatake, N. Structure–Sweetness Relationship in Egg White Lysozyme: Role of Lysine and Arginine Residues on the Elicitation of Lysozyme Sweetness. *Chem. Senses* **2005**, 30, 667–681.

(31) Chen, D.; Disotuar, M. M.; Xiong, X.; Wang, Y.; Chou, D. H.-C. Selective N-Terminal Functionalization of Native Peptides and Proteins. *Chem. Sci*. **2017**, 8, 2717–2722.

(32) Guerry, A.; Bernard, J.; Samain, E.; Fleury, E.; Cottaz, S.; Halila, S. Aniline-Catalyzed Reductive Amination as a Powerful Method for the Preparation of Reducing End-"Clickable" Chitooligosaccharides. *Bioconjug. Chem*. **2013**, 24, 544–549.

(33) Presolski, S. I.; Hong, V. P.; Finn, M. G. Copper-Catalyzed Azide–Alkyne Click Chemistry for Bioconjugation. *Curr. Protoc. Chem. Biol*. **2011**, 3, 153–162.

(34) Stayton, P. S.; Shimoboji, T.; Long, C.; Chilkoti, A.; Ghen, G.; Harris, J. M.; Hoffman, A. S. Control of Protein–Ligand Recognition Using a Stimuli-Responsive Polymer. *Nature* **1995**, 378, 472–474.

(35) Fuhrmann, G.; Grotzky, A.; Lukić, R.; Matoori, S.; Luciani, P.; Yu, H.; Zhang, B.; Walde, P.; Schlüter, A. D.; Gauthier, M. A.; Leroux, J.-C. Sustained Gastrointestinal Activity of Dendronized Polymer–Enzyme Conjugates. *Nat. Chem*. **2013**, 5, 582–589.

TOC:

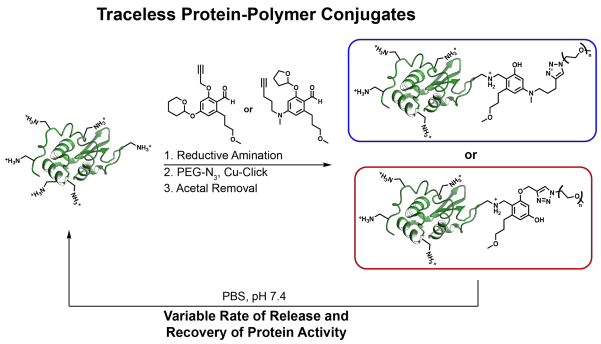
Traceless Protein-Polymer Conjugates
or
1. Reductive Amination
2. PEG-N3, Cu-Click
3. Acetal Removal
or
PBS, pH 7.4
Variable Rate of Release and
Recovery of Protein Activity